Bioresource Technology 289 (2019) 121724

Contents lists available at ScienceDirect

Bioresource Technology

journal homepage: www.elsevier.com/locate/biortech

Quantitative Structure-Toxicity Relationship analysis of combined toxic effects of lignocellulose-derived inhibitors on bioethanol production

Jinju Hou[a], Jiawen Tang[a,b], Jinhuan Chen[a,b], Qiuzhuo Zhang[a,b,*]

[a] Shanghai Key Lab for Urban Ecological Processes and Eco-Restoration, School of Ecological and Environmental Sciences, East China Normal University, 200241 Shanghai, China

[b] Institute of Eco-Chongming (IEC), 3663 N. Zhongshan Rd., Shanghai 200062, China

GRAPHICAL ABSTRACT

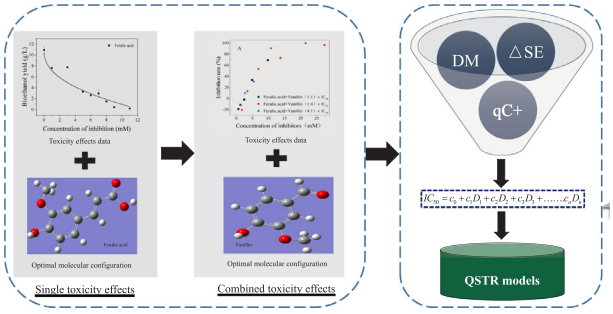

ARTICLE INFO

Keywords:
QSTR
Combined toxic effects
Lignocellulose-derived inhibitors
Ferulic acid

ABSTRACT

This study performed a Quantitative Structure-Toxicity Relationship (QSTR) model to evaluate the combined toxicity of lignocellulose-derived inhibitors on bioethanol production. Compared with all the control groups, the combined systems exhibited lower conductivity values, higher oxidation-reduction potential values, as well as maximum inhibition rates. These results indicated that the presence of combined inhibitors had a negative effect on the bioethanol fermentation process. Meanwhile, QSTR model was excellent for evaluating the combined toxic effects at lower ferulic acid concentration (([1:4] × IC50)) and (([1:1] × IC50)), due to higher R^2 values (0.994 and 0.762), lower P values (0.000 and 0.023) and relative error values (less than 30%). The obtained results also showed that the combined toxic effects of ferulic acid and representative lignocellulose-derived inhibitors were relevant to different molecular descriptors. Meanwhile, the interactions of combined inhibitors were weaker when ferulic acid was at low concentration ([1:4] × IC50).

1. Introduction

Due to the increasingly serious energy crisis and environmental pollution, renewable bioethanol has become a potential alternative to fossil energy (Lopez-Hidalgo et al., 2017; Zhao et al., 2015). Compared with traditional fossil fuels, bioethanol possesses many favorable combustion characteristics, such as higher vaporization heats, broader flammability limits and faster flame speeds (Chen and Fu, 2016). In recent years, the abundant non-food lignocellulose biomass, which is obtained from crop straw, has arisen as promising raw material for bioethanol production (Shin et al., 2017; Szambelan et al., 2018). To obtain a high conversion rate of bioethanol from lignocellulose

* Corresponding author at: Shanghai Key Lab for Urban Ecological Processes and Eco-Restoration, School of Ecological and Environmental Sciences, East China Normal University, 200241 Shanghai, China.
E-mail address: qzhzhang@des.ecnu.edu.cn (Q. Zhang).

https://doi.org/10.1016/j.biortech.2019.121724
Received 7 May 2019; Received in revised form 26 June 2019; Accepted 28 June 2019
Available online 01 July 2019
0960-8524/

biomass, a pretreatment process is performed to degrade stable lignocellulose structure, thus ensuring the efficiency of subsequent fermentation (Liu et al., 2016). However, the key challenge for the pretreatment process is that it is accompanied by the formation of substantial amounts of lignocellulose-derived inhibitors (LDIs). These inhibitors, which can be broadly divided into phenols, weak acids and furans (Kim et al., 2015; Saravanakumar et al., 2016), can inhibit bioethanol fermentation if their concentration exceeds the tolerance range of the microorganism (Shin et al., 2017). Therefore, their removal increases terminal bioethanol yield in the hydrolysates.

The fermentative microorganisms that exist in practical hydrolysates are usually exposed to various kinds of LDIs together (Chen and Wan, 2017; Wang et al., 2017). Compared with single inhibitors alone, these inhibitory mixtures might contribute to different interactions affecting microbial fermentation. It has been shown previously that the interactions between acetic acid and furfural on *Saccharomyces cerevisiae* are mainly synergistic, whereas obvious antagonism was observed between formic acid and 5-hydroxymethyl furfural (Larsson et al., 1999; Palmqvist and Hahn-Hägerdal, 2000). It was also found that the interactions between phenols and the other fermentation inhibitors could mostly be characterized as synergistic (Larsson et al., 1999; Palmqvist and Hahn-Hägerdal, 2000). Generally, different combined toxic effects have been shown by various combinations of fermentation inhibitors.

In the fermentation broth of bioethanol production process, various kinds of LDIs were co-existed after pretreatment, which could lead a decline for bioethanol production eventually. It was shown that the application of individual inhibitor based on toxicity data was not so accurate to evaluate the interactions and the related inhibitory effects of fermentation inhibitors in mixtures (Jin et al., 2014; Su et al., 2012). Therefore, it is essential to develop new tools to understand, explain and predict the combined toxic effects of fermentation inhibitors in the hydrolysate on bioethanol production (Hou et al., 2019; Wang et al., 2018; Xu and Nirmalakhandan, 1998).

Quantitative Structure-Toxicity Relationship (QSTR) modeling has successfully been used to explain the correlations between the molecular descriptors of chemicals and their toxicity (Jia et al., 2015; Tugcu et al., 2017). It has been widely used in many fields to predict the individual toxicity of chemicals (Bao et al., 2012; Roy and Das, 2013), however, it was rarely used for the prediction of combined toxic effects. Many previous studies demonstrated that the prediction of combined toxicity was inaccurate because they were only based on using simple additive effect method (Su et al., 2012). Meanwhile, the mixed ratios of different fermentation inhibitors, which might cause different toxicity response, were not in consideration (Kungolos et al., 2009; SU et al., 2008; Su et al., 2010). These results can lead to under- or over-estimation of the combined effects of co-existing inhibitors (Nirmalakhandan et al., 1997; Shen et al., 2006). The application of QSTR modeling might be beneficial to explain the above phenomena by establishing models based on observed different combined toxicity, which is the major difficulty of QSTR model applied in fermentation field currently.

Ferulic acid was the most toxic fermentation inhibitor in alkali-pretreated rice straw hydrolysates in the previous research (Hou et al., 2018; Zhang et al., 2017). Considering the complexity of the actual pretreatment hydrolysate, the combined toxicity between ferulic acid and other inhibitors was preliminarily analyzed by additive index (AI) methods based on our experimental data (Hou et al., 2019). The results indicated that ferulic acid played an important role in the combined toxicity. However, the combined toxic effects were different in various kinds of pretreated hydrolysates. Therefore, deep analysis of the mechanisms of toxicity may be necessary to elucidate combined toxic effects by the assistance of QSTR models using ferulic acid as research objective.

In this study, various inhibitor combinations in different mixture ratios, including ferulic acid and the other representative LDIs, were chosen for (i) analyzing the combined toxicity of ferulic acid and the other representative LDIs on the growth of *Saccharomyces cerevisiae* (*S. cerevisiae*) and bioethanol production (ii) evaluating the combined toxicity of ferulic acid with the other representative LDIs at different mixed ratios; (iii) investigating the correlation between combined toxicity of fermentation inhibitors and calculated molecular descriptors, as well as establishing QSTR models at different mixed ratios; (IV) exploring the combined toxicity mechanisms by established QSTR models.

2. Materials and methods

2.1. Inhibitors and microorganisms

Based on known toxic effects of single inhibitors on bioethanol production, LDIs including vanillin (purity ≥ 98%), syringaldehyde (purity > 99%), 4-hydroxybenzaldehyde (purity ≥ 98%), vanillic acid (purity ≥ 98%), ferulic acid (purity ≥ 98%) (phenols), formic acid (purity ≥ 98%) (weak acids), and furfural (purity > 99%) (furans), were prepared for the experiment (Hou et al., 2017; Hou et al., 2018). They were all of high purity and were obtained from Sinopharm Chemical Reagent Co., Ltd., China.

S. cerevisiae, which was used in the fermentation process, was provided by the China Center of Industrial Culture Collection (CICC). It was stored at 4 ℃ for the subsequent fermentation experiment.

2.2. Evaluating the toxic effects of represented LDIs on the fermentation process

S. cerevisiae was activated in 100 mL YPG broth at 30 ˚C prior to the toxicity experiment. Once the microorganism reached the logarithmic growth phase, the culture was centrifuged at 4000 rpm for 5 min and prepared for cell suspensions. To monitor the combined toxicity of ferulic acid and the other LDIs on the fermentation process in real time, the main representative LDIs, which included phenols (vanillin), weak acids (formic acid), and furans (furfural), were mixed with ferulic acid at the same concentration (1:1) × IC_{50} (median lethal concentration) (Group A) and dilution level (0.5:0.5) × IC_{50} (diluted two-fold) (Group B). All of the IC_{50} values of the experimental chemicals were obtained from individual toxicity experiments based on the previous research results (Hou et al., 2019). Different concentrations of the combined inhibitors were added to the fermentation medium at 40 ˚C (165 rpm). The medium contained 0.8 g/L cell suspensions. To investigate the combined toxic effects of fermentation inhibitors on the bioethanol fermentation process preliminarily and monitor changes in the fermentation system in real time, the fermentation broth was taken out at a succession of times (0, 4, 8, 16, 36, 72, 144, and 216 h), in order to determine conductivity, oxidation-reduction potential (ORP) and pH. It was worth noting that conductivity value was used to describe the ability of substances to transmit current electricity, which could reflect the concentration of electrolytes in fermentation broth. Conductivity and ORP values were measured using a conductivity meter (HPD-50, China), and the pH value was detected by a pH meter (PHS-3C, China). All toxicity experiments were performed in triplicate.

2.3. Evaluating the toxic effects of represented LDIs on bioethanol yield

In order to study combined toxic effects on bioethanol yield, representative LDIs (vanillin, furfural, 4-hydroxybenzaldehyde syringaldehyde, vanillic acid, and formic acid) and ferulic acid were mixed at different concentration ratios (1:4, 1:1, and 4:1) × IC_{50}, respectively, representing low, medium, and high levels of ferulic acid. The obtained combined concentrations at the above different ratios were diluted continuously by the same dilution factor (two-fold). Finally, five consecutive concentration gradients of combined inhibitors at each ratio were obtained, and the combined toxicity data were measured to

prepare the inhibition rate curves using gas chromatography (GC, Agilent 7890A, USA) accompanied by headspace sampling (automatic headspace sampler HS-9A, Sida Analytic Instruments Co., Ltd, China). The IC_{50} values of different mixture combinations were calculated based on the obtained inhibition rate curves, which were used to establish the different QSTR models. The measurement method of the combined toxicity data was the same as that of single toxicity data (Hou et al., 2019).

2.4. Acquisition of molecular descriptors for QSTR models

Molecular descriptors, which were used to reflect the physicochemical properties of chemicals, were calculated from their respective molecular structures using the quantum chemical modules of GAUSSIAN 09 and CHEMBIOOFFICE 2012 software (Meng-Lund et al., 2018). All molecules of inhibitors were optimized at the level of b3lyp/6–31 + g (d, p). Structural energy minimizations were then obtained to calculate molecular descriptors (Karabulut et al., 2016). The extracted corresponding molecular descriptors were expressed as follows: molecular orbital parameters (E_{SHOMO} [the secondary highest occupied orbital energy of molecules], $\triangle$SE [the secondary frontier orbital energy differences]), electrostatic parameters (ω [the electrophilic index], qC^+ [the maximum positive charge number on a carbon atom], TC [the total electrical charge number of carbon atoms]), and polarity/dipole/volume/space parameters (DM [the dipole moment], ESE [the electron space]). These parameters can be used to predict the reactivity of inhibitor molecules and their ability to bind to receptors (Hou et al., 2018).

2.5. Data analysis of QSTR models

Multiple linear regression analysis was performed using SPSS 22.0 software to establish the QSTR models of various combined toxic effects at different mixture ratios. The obtained mathematical equations were used to explain the relationship between the combined toxic effects and molecular physico-chemical properties. The utility of the established QSTR models was characterized by coefficient of determination (R^2), standard error of estimate (SE), Fischer ratio (F), variance inflation factor (VIF), and significance level (P). The VIF values were used to assess multicollinearity among the variables.

3. Results and discussion

3.1. The combined toxic effects of fermentation inhibitors on the bioethanol fermentation process

The conductivity, ORP and pH values in the fermentation broth were shown in Fig. 1. Conductivity values were used to reflect the growth of *S. cerevisiae* (Zhang et al., 2017). ORP reflected the redox properties of fermentation broth. The higher value of the redox potential indicated the stronger ability of the oxidation process. The ORP value played an important role in the response of cell growth and metabolism (Lin et al., 2005; Sizer, 1942). Additionally, pH value was an important indicator which could affect the yeast metabolic fermentation (Feng et al., 2018). The measurement of these parameters was of great significance to explore the role of fermentation inhibitors in bioethanol production.

The conductivity values of all control (CK) groups increased rapidly as fermentation proceeded, whereas there were no obvious differences among the different combined systems. Compared with the combined systems, the CK groups exhibited higher conductivity values, which might be because *S. cerevisiae* in this group grew in large numbers and produced more metabolites (Bryant et al., 2011; Zhang et al., 2017). However, the combined systems showed basically stable conductivity values due to the weak metabolic activities of *S. cerevisiae*, which led to the reduction of the utilization of nutrients as well as the production of metabolites. Additionally, the higher fermentation performance of CK groups increased the content of fiber fines in amorphous region, which caused the increase of the conductivity values of fermentation medium (Khalil et al., 2017).

Overall, these data indicated that the combined inhibitors had negative effects on the growth of *S. cerevisiae*, which would influence the bioethanol fermentation process and cause the reduction of bioethanol production eventually. However, before 25 h, the conductivity values of group A (Fig. 1 B) were slightly higher than the CK group, which was probably due to the addition of combined inhibitors causing intracellular substances to release into the fermentation broth, thus temporarily increasing the conductivity values (Bryant et al., 2011). Additionally, it was found that the conductivity values of group B (Fig. 1B) were slightly higher than those of group A, which because the high-concentration metabolites and bioethanol were presented in this fermentation broth (Bryant et al., 2011; Zhang et al., 2017).

Along with the rapid growth of *S. cerevisiae*, the ORP values of all CK groups and combined systems decreased sharply, because the growth of yeast cells consumed the dissolved oxygen in fermentation broth and produced nicotinamide adenine dinucleotide (NADH) (Bakker et al., 2001). However, compared with the combined systems, the CK groups could maintain relatively lower ORP values. Previous researches showed that the high ORP values were beneficial to produce glycerol by the consumption of NADH, while inhibited the conversion of sugars into bioethanol (Alfenore et al., 2004; van Dijken and Scheffers, 1986). Compared to CK groups, the higher ORP values in the combined systems also indicated that the combined inhibitors had negative effects on bioethanol production. Before 150 h, the ORP values of group B (Fig. 1E and F) were slightly higher than those of group A, which might be because of stimulatory effects of inhibitors in the early fermentation process (Stebbing, 2002). With the onset of the declining phase of *S. cerevisiae* growth, it was found that ORP values were slightly higher in group A than that in group B, which indicated that small quantities of NADH were existed in yeast cells and cells were entered to a decline phase (Bakker et al., 2001). These results showed that higher combined inhibitor concentration (group A) exhibited a negative effect on the growth of *S. cerevisiae*, thus influencing the subsequent bioethanol fermentation.

The pH values of the CK groups were highly increased after 50 h fermentation, due to increased numbers of alkaline functional groups, principally hydroxyl groups, resulting from bioethanol production. Furthermore, the pH value between 5 and 5.5 in CK groups was more suitable for *S. cerevisiae* fermentation. All of these indicated that the stronger fermentation capacity of CK groups (Saha et al., 2019). However, the pH levels of all of the combined groups remained almost constant, and they were lower than of the CK groups. These results reflected the relatively weak fermentation capacity of the combined systems compared to CK groups, resulting in less production of alkaline functional moieties (bioethanol) in these groups. These results also indicated that the presence of combined inhibitors had a negative effect on the bioethanol fermentation process. Additionally, Tang et al. (2017) showed that pH played an important role in dominating the fermentation type and the production yield of byproducts due to the enzymatic activity, and metabolic pathway were influenced by pH. Wu et al. (2015) found that the main target product from agricultural wastes at pH 4.0 was lactic acid. However, when the pH value was larger than 5, it would be beneficial to the production of bioethanol due to the strong absorption of nutrients and high activity of metabolic enzymes (Saha et al., 2019). Thus, it was indicated that the bioethanol fermentation of CK groups (pH > 5) was better than that of the combined systems.

3.2. The combined toxic effects of fermentation inhibitors on bioethanol yield

In order to precisely evaluate the combined toxic effects of various LDIs on bioethanol yield, and obtain the toxic effects data needed to

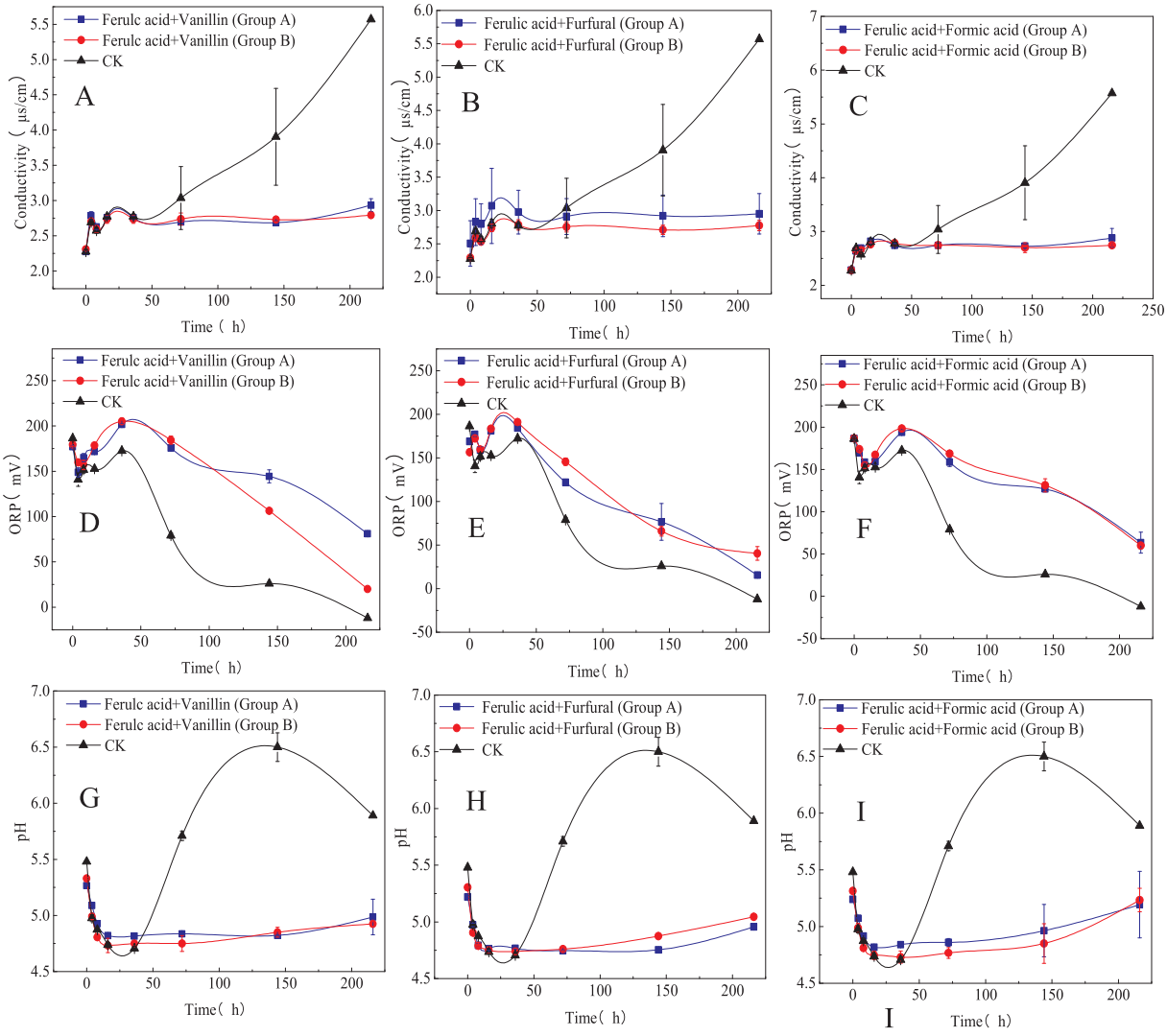

Fig. 1. Conductivity, ORP, and pH of (A, D, G) Vanillin, (B, E, H) Furfural, (C, F, I) Formic acid curves with ferulic acid using *S. cerevisiae* fermentation at different mixed ratios. *Legends:* Vanillin, Formic acid, and Furfural, were mixed with ferulic acid at the different mixed ratios of ([1:1] × IC_{50}) (Group A) (■), ([0.5:0.5] × IC_{50}) Group B) (●), and control (CK) group (▲), respectively.

establish the QSTR models, the combined toxic effects of ferulic acid and various LDIs, including phenols (vanillin, syringaldehyde, and vanillic acid), weak acids (formic acid) and furans (furfural), were investigated for their effect on bioethanol yield (Fig. 2). These toxicity data acquisition methods were as described in the previous studies (Hou et al., 2019). Additionally, the fermentation experiments including all the combined inhibitors were performed under the same experimental conditions. It was found that the inhibition rates of bioethanol yield increased distinctly after adding different combined inhibitors (Fig. 1; Fig. 2). It was also noted that only lower concentrations of combined inhibitors could be used to achieve optimal inhibition rates at higher ratios of ferulic acid. This indicated that combined toxic effects had a positive correlation with ferulic acid concentration in combined inhibitors. The inhibition rates were used to describe the combined toxic effects. By comparing the maximum inhibition rates of different combined inhibitors between ferulic acid and various LDIs, including phenols (vanillin [69.3%, 96.4%, and 99.8%], syringaldehyde [79.2%, 96.7%, and 99.9%], 4-Hydroxybenzaldehyde [75.8%, 98.9%, and 100%], and vanillic acid [70.3%, 90.7%, and 100%]), weak acid (formic acid [100%, 100%, and 100%]), and furan (furfural [98.7%, 100%, and 100%]) at different inhibitors mixture ratios (1:1, 1:4, and 4:1), respectively. It was found that the maximum inhibition rates of combined inhibitors obtained from Fig. 2 were positively related to different mixture ratios.

The combined inhibitors produced the combined toxic effects by affecting the growth and metabolism of *S. cerevisiae*. The higher concentration and mixed ratios of ferulic acid in the mixtures presented the stronger combined toxic effects, because ferulic acid had the strongest toxicity compared to the other representative LDIs (Zhang et al., 2017). Mills et al. (2009) showed that the growth of *S. cerevisiae* was affected by the change of utilization pathway of nutrients. Fermentation inhibitors have also proven to produce toxicity by the ortho-electron-withdrawing functional groups, including carbon-carbon double bond and hydroxyl group (Hou et al., 2017; Hou et al., 2018). Meanwhile, the types and positions of functional groups played an important role in dominating the toxicity by destroying the cell membrane and antioxidant defense systems of *S. cerevisiae* (Andary et al., 2013; Saravanakumar et al., 2016). To study the toxicity mechanism specifically, the IC_{50} values of different mixture combinations were calculated based on the obtained inhibition rate curves. These values were used to establish the QSTR models subsequently.

3.3. Establishment of QSTR models

QSTR models were established to evaluate the combined toxic effects of ferulic acid and the other representative LDIs at different

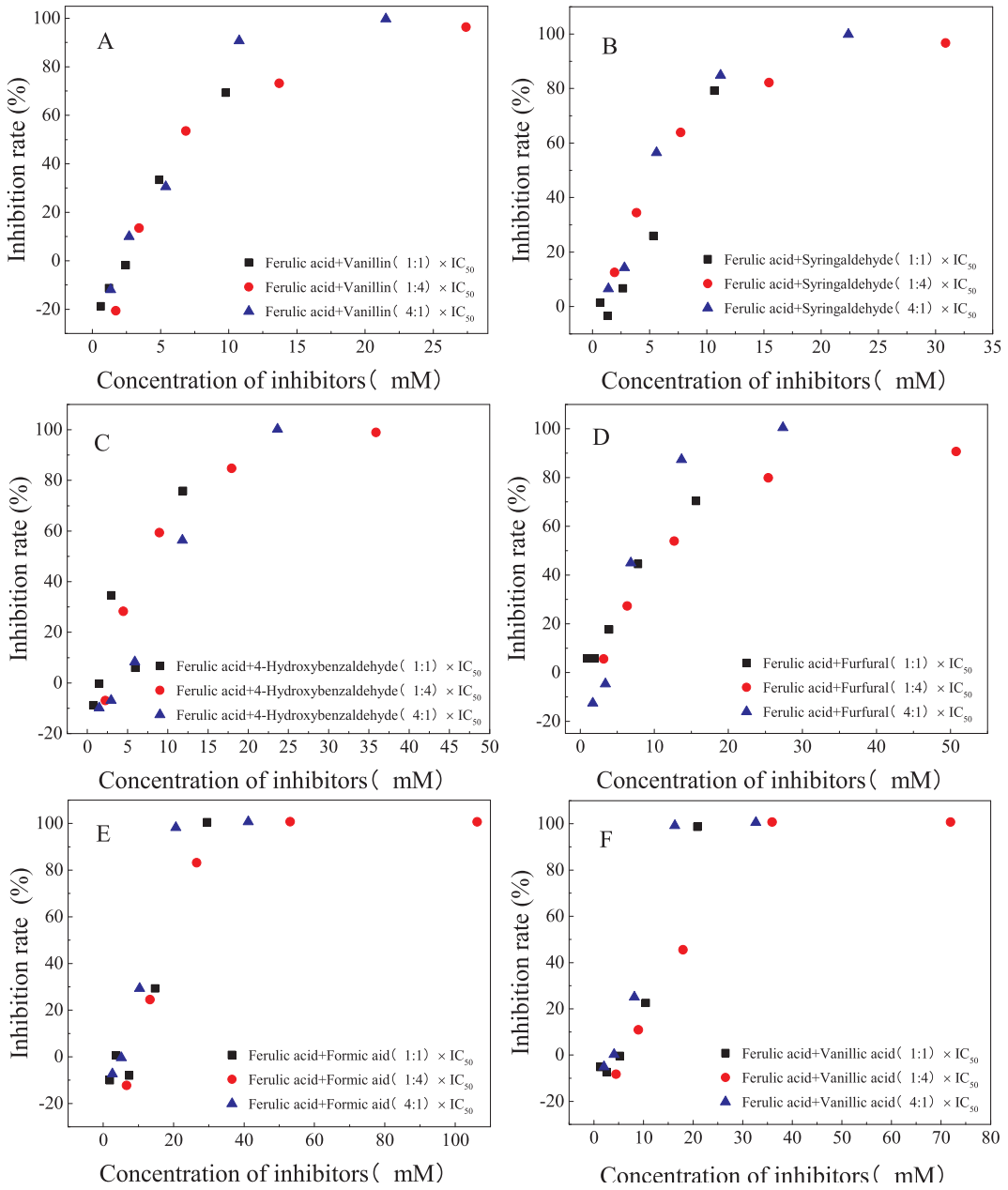

Fig. 2. Inhibition data of (A) Vanillin, (B) Syringaldehyde, (C) 4-Hydroxybenzaldehyde, (D) Furfural, (E) Formic acid, (F) Vanillic acid curves with ferulic acid using *S. cerevisiae* fermentation at different mixed ratios. *Legends:* Vanillin, Syringaldehyde, 4-Hydroxybenzaldehyde, Furfural, Formic acid, and Vanillic acid, were mixed with ferulic acid at the different mixed ratios of (1:1) × IC_{50} (■), (1:4) × IC_{50} (●), (4:1) × IC_{50} (▲), respectively.

Table 1
QSTR models and fitting parameters for single and combined toxic effects of fermentation inhibitors.

Model Equation	QSTR models	Model parameters					
		n	R^2	SE	P	F	VIF
1	$IC_{50} = -61.323 + 23.476 \times qC^{+} - 143.175 \times \Delta SE$	6	0.970	1.696	0.005	48.814	(1.309, 1.309)
2	$IC_{50} = -94.329 + 43.095 \times qC^{+} - 162.208 \times \Delta SE$	6	0.994	0.939	0.000	242.451	(1.309, 1.309)
3	$IC_{50} = 18.479 - 1.866 \times DM$	6	0.762	1.941	0.023	12.790	1.000
4	$IC_{50} = 13.998 - 1.194 \times DM$	6	0.519	2.141	0.106	4.311	1.000

mixture ratios. Stepwise regression was used to develop the QSTR models at low, medium, and high mixture ratios (1:4, 1:1, and 4:1) × IC_{50} of ferulic acid. It is notable that the QSTR models of combined toxic effects were built using the same molecular descriptors as single toxicity models at different mixture ratios. The model equations of single and combined toxic effects of the representative LDIs and ferulic acid are shown in Table 1. These were used to describe the QSTR models of single toxic effects of the other representative LDIs, as well as those of combined toxicity effects with low, medium, and high ferulic acid concentrations (Eqs. (1)–(4)).

Table 2
Molecular descriptors of lignocellulose-derived inhibitors of different mixed ratios and relative errors between experimental and predicted values.

No.	Inhibitors	Molecular descriptors			Relative errors (%)			
		qC^+	△SE	DM	Eq. (1)	Eq. (2)	Eq. (3)	Eq. (4)
1	Vanillin	1.424	−0.248	6.685	−29.648	−6.366	8.1	8.417
2	Syringaldehyde	1.425	−0.240	4.453	24.327	−4.392	−48.9	−64.946
3	Vanillic acid	1.846	−0.390	3.493	2.085	0.048	12.7	0.844
4	4-Hydroxybenzaldehyde	1.406	−0.296	4.518	−10.018	18.905	5.6	22.323
5	Formic acid	1.301	−0.244	1.818	0.289	1.406	0.1	3.619
6	Furfural	1.356	−0.239	5.456	5.827	−7.995	5.3	−2.039

It was found from Eqs. (1) to (4) that the QSTR model, which was developed at a low ratio of ferulic acid with the representative LDIs ([1:4] × IC_{50}) (Eq. (2)), was similar to that of single toxicity of the representative LDIs (Eq. (1)). The same molecular descriptors that appeared in Eqs. (1) and (2), indicated that the interactions between ferulic acid and the other representative LDIs were weak at low ferulic acid concentration (Su et al., 2012). Meanwhile, their combined toxic effects had a linear relationship with the single toxic effects of the representative LDIs, which could be calculated by the appropriate addition of single toxicity of ferulic acid and the representative LDIs. In the previous study, it was found that this simple additive effect was mainly apparent with low ferulic acid concentration (Hou et al., 2019). The results of this earlier study also confirmed that QSTR models could be used to predict the simple additive effect with the assistance of the different interaction results. The molecular descriptors of the representative LDIs and their relative errors calculated from Eqs.(1) to (4) are listed in Table 2. As shown in Table 2, it was found that the 85% relative error values obtained from Eqs. (3) and (4), remained that did not differ by more than 30%, while all of the relative error values were smaller than 30% in Eqs. (1) and (2).

It is notable that the model quality of Eq. (4) was inferior to Eqs. (1)–(3). The established QSTR models were evaluated by their regression parameters. The R^2 values of Eqs. (1)–(3) were larger than 0.6, and their SE values were relatively small. Significance testing, performed to assess the accidental errors, indicated that these were relatively small ($P < 0.05$) for Eqs. (1)–(3). Meanwhile, the VIF values of Eqs. (1)–(3) were smaller than 10, which indicated acceptable multicollinearity (Ghamali et al., 2017; Masand et al., 2017). However, the R^2 values of Eq. (4) were relatively small, and the P values of Eq. (4) were larger than 0.05.

The above results indicated that the QSTR models were poor for evaluating the combined toxic effects between ferulic acid and the other representative LDIs at high ferulic acid concentrations. It might be due to increased antagonistic interactions between inhibitors (Hou et al., 2019). Compared with the promising availabilities of QSTR models for evaluating the simple additive effect, these results also confirmed that the prediction of the combined toxicity of antagonistic effects using a simple additive effect method was inaccurate, and the different combined toxic effects should be evaluated using the specific methods.

3.4. Insights into the mechanisms of the combined toxic effects from QSTR analysis

The predicted values obtained from the models represented in Eqs. (1)–(3) were plotted against the experimental values (Fig. 3). The data points were evenly distributed near the diagonals, indicating that the experimental values were consistent with the predicted values (Burden et al., 2016). This was confirmed by the obtained R^2 (0.983) and P values (< 0.0001), indicating that the above three QSTR models could be used to predict the combined toxic effects of representative LDIs with ferulic acid (Su et al., 2012).

Additionally, the established QSTR models could be used to gain insight into the mechanisms of toxicity, based on the molecular descriptors in these models. It was shown in Eqs. (1)–(3) that the combined toxic effects of representative LDIs and ferulic acid were closely related to the molecular orbital parameters, the electrostatic parameters, and the dipole moment at low and medium ferulic acid mixture concentrations. △SE in Eqs. (1) and (2) indicated that the energy required for electron transfer positively correlated with reactivity (Hou et al., 2018). The negative equation coefficients (−106.854, −143.175, and −162.208), which were obtained from these models, implied that higher values of △SE were obtained, and that lower combined toxic effects were present. This was probably due to the higher △SE required more energy in the reaction process, which increased the difficulty of reaction between combined inhibitors and *S. cerevisiae*, decreased the electrophilic reactivity or nucleophilic reactivity, thus reducing the combined toxic effects of inhibitors on microbial fermentation (Hou et al., 2018).

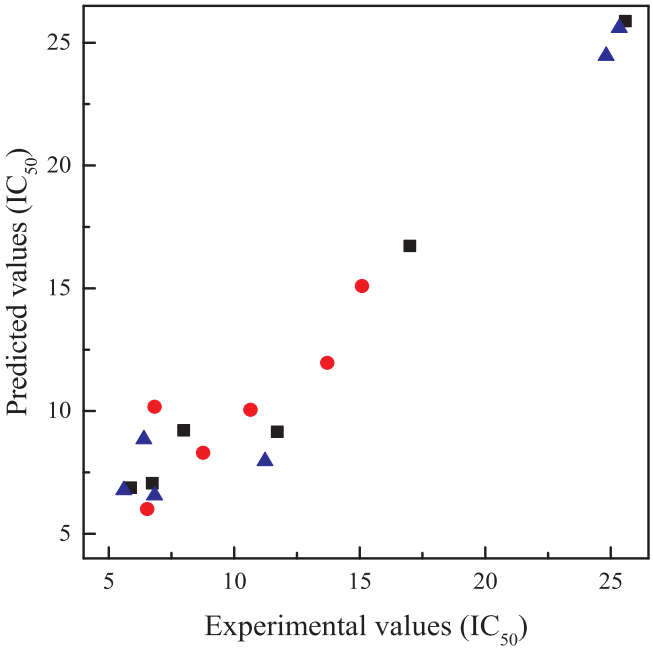

Fig. 3. Diagram of experimental values against predicted values of binary co-existed inhibitors. *Legends:* Eq. (1) (■), Eq. (2) (●), Eq. (3) (▲) were used to describe the QSTR models of single toxic effects of the other representative LDIs, as well as those of combined toxic effects with low, and medium ferulic acid concentrations.

Eqs. (1) and (2), indicated that the combined toxic effects of representative LDIs and ferulic acid were correlated with the number of maximum positive charges on carbon atoms (qC^+). This molecular descriptor was used to describe the charge distribution of inhibitor molecules, which reflected their electrostatic characteristics (Yong-Ling et al., 2017). The positive coefficient of qC^+ in the above two models demonstrated that a larger number of charges on carbon atoms per molecule was associated with stronger toxic effects of combined inhibitors on bioethanol production. This was presumably due to the

stronger nucleophilic reactivity of combined inhibitors towards the intracellular structures of *S. cerevisiae* (Andary et al., 2013), which inhibited the normal metabolism of fermentative microbes, and reduced their bioethanol production eventually.

It was found that, compared with Eqs. (1)–(2) and Eq. (3), DM, which was used to describe the binding affinity of carbonyl site in ferulic acid, was more negatively related to the stepwise regression model in Eq. (3) than the other molecular descriptors. DM could be used to reflect the differences in electronegativity due to the presentation of functional groups of C═O (Yong-Ling et al., 2017). This result might be because of the interactions between combined inhibitors increasing at higher ferulic acid concentrations, resulting in increased binding capacity of ferulic acid with the representative LDIs instead of *S. cerevisiae*, thus decreasing the overall combined toxic effects of the combined inhibitors. These toxicity mechanisms could be used to explain the phenomena of underestimation of the antagonistic effects using a simple additive effect method. This phenomena might be due to the interactions of binding capacity between combined inhibitors increasing at higher ferulic acid concentrations, thus reducing the effective number of combined inhibitors that react with *S. cerevisiae*, and resulting in underestimation of the toxicity of the antagonistic effects (Lopez-Hidalgo et al., 2017). The obtained results in the manuscript were consistent with many previous researches and could provide a good supplement for the previous study (Hou et al., 2017; Hou et al., 2018; Hou et al., 2019; Zaldivar et al., 2000).

These obtained results also provided the theoretical guidance for the removal of representative LDIs and ferulic acid. The following measures should be taken to reduce the combined toxic effects of inhibitors, thus increasing the bioethanol production eventually. (i) Reduce the concentration of ferulic acid in pretreated hydrolysate considering its dominant function of combined toxic effects. (ii) Optimize the pretreatment conditions to avoid the presence of some stronger toxic inhibitors. (iii) Explore the new adsorbents to bind with the reaction sites of fermentation inhibitors for reducing their effective reaction with *S. cerevisiae*. (iv) Screen the resistant fermentation strains.

4. Conclusions

QSTR models of ferulic acid and various representative LDIs were built at different concentration ratios. These models were useful for evaluating the combined toxic effects at low and medium ferulic acid concentrations. Results showed that the combined toxic effects were mainly related to the number of maximum positive charges on carbon atoms, the secondary frontier orbital energy differences and the dipole moment. Because various LDIs were co-existed in pretreated lignocellulosic hydrolysates, integrated toxicity of more than three inhibitors would be investigated in the future research based on the obtained experimental results.

Acknowledgments

This project is funded by the National Key R&D Program of China [2018YFC1901005], Shanghai Science and Technology Committee [No. 17295810603, 17DZ1202804, and 18295810400], and the Institute of Eco-Chongming [ECNU-IEC-201901]. The authors would like to thank them for funding this work.

Declaration of Competing Interest

None.

References

Alfenore, S., Cameleyre, X., Benbadis, L., Bideaux, C., Uribelarrea, J.-L., Goma, G., Molina-Jouve, C., Guillouet, S.E., 2004. Aeration strategy: a need for very high ethanol performance in *Saccharomyces cerevisiae* fed-batch process. Appl. Microbiol. Biotechnol. 63 (5), 537–542.

Andary, J., Maalouly, J., Ouaini, R., Chebib, H., Beyrouthy, M., Rutledge, D.N., Ouaini, N., 2013. Phenolic compounds from diluted acid hydrolysates of olive stones: effect of overliming. Adv. Crop. Sci. Technol. 01 (1), 103.

Bakker, B.M., Overkamp, K.M., van Maris, A.J.A., Kötter, P., Luttik, M.A.H., van Dijken, J.P., Pronk, J.T., 2001. Stoichiometry and compartmentation of NADH metabolism in *Saccharomyces cerevisiae*. Fems. Microbiol. Rev. 25 (1), 15–37.

Bao, Y., Huang, Q., Li, Y., Li, N., He, T., Feng, C., 2012. Prediction of nitrobenzene toxicity to the algae (*Scenedesmus obliguus*) by quantitative structure–toxicity relationship (QSTR) models with quantum chemical descriptors. Environ. Toxicol. Pharmacol. 33 (1), 39–45.

Bryant, D.N., Morris, S.M., Leemans, D., Fish, S.A., Taylor, S., Carvell, J., Todd, R.W., Logan, D., Lee, M., Garcia, N., Ellis, A., Gallagher, J.A., 2011. Modelling real-time simultaneous saccharification and fermentation of lignocellulosic biomass and organic acid accumulation using dielectric spectroscopy. Bioresour. Technol. 102 (20), 9675–9682.

Burden, N., Maynard, S.K., Weltje, L., Wheeler, J.R., 2016. The utility of QSARs in predicting acute fish toxicity of pesticide metabolites: a retrospective validation approach. Regul. Toxicol. Pharmacol. 80, 241–246.

Chen, H., Fu, X., 2016. Industrial technologies for bioethanol production from lignocellulosic biomass. Renew. Sustain. Energy Rev. 57, 468–478.

Chen, Z., Wan, C., 2017. Co-fermentation of lignocellulose-based glucose and inhibitory compounds for lipid synthesis by *Rhodococcus jostii RHA1*. Process Biochem. 57, 159–166.

Feng, K., Li, H., Zheng, C., 2018. Shifting product spectrum by pH adjustment during long-term continuous anaerobic fermentation of food waste. Bioresour. Technol. 270, 180–188.

Ghamali, M., Chtita, S., Ousaa, A., Elidrissi, B., Bouachrine, M., Lakhlifi, T., 2017. QSAR analysis of the toxicity of phenols and thiophenols using MLR and ANN. J. Taibah Univ. Sci. 11 (1), 1–10.

Hou, J., Ding, C., Qiu, Z., Zhang, Q., Xiang, W.-N., 2017. Inhibition efficiency evaluation of lignocellulose-derived compounds for bioethanol production. J. Clean Prod. 165, 1107–1114.

Hou, J., Qiu, Z., Han, H., Zhang, Q., 2018. Toxicity evaluation of lignocellulose-derived phenolic inhibitors on *Saccharomyces cerevisiae* growth by using the QSTR method. Chemosphere 201, 286–293.

Hou, J., Tang, J., Chen, J., Deng, J., Wang, J., Zhang, Q., 2019. Evaluation of inhibition of lignocellulose-derived by-products on bioethanol production by using the QSAR method and mechanism study. Biochem. Eng. J. 147, 153–162.

Jia, L., Shen, Z., Guo, W., Zhang, Y., Zhu, H., Ji, W., Fan, M., 2015. QSAR models for oxidative degradation of organic pollutants in the Fenton process. J. Taiwan Inst. Chem. E 46, 140–147.

Jin, H., Wang, C., Shi, J., Chen, L., 2014. Evaluation on joint toxicity of chlorinated anilines and cadmium to *Photobacterium phosphoreum* and QSAR analysis. J. Hazard. Mater. 279, 156–162.

Karabulut, S., Sizochenko, N., Orhan, A., Leszczynski, J., 2016. A DFT-based QSAR study on inhibition of human dihydrofolate reductase. J. Mol. Graph Model. 70, 23–29.

Khalil, A.M., Hassan, M.L., Ward, A.A., 2017. Novel nanofibrillated cellulose/polyvinylpyrrolidone/silver nanoparticles films with electrical conductivity properties. Carbohyd. Polym. 157, 503–511.

Kim, S.-K., Jin, Y.-S., Choi, I.-G., Park, Y.-C., Seo, J.-H., 2015. Enhanced tolerance of *Saccharomyces cerevisiae* to multiple lignocellulose-derived inhibitors through modulation of spermidine contents. Metab. Eng. 29, 46–55.

Kungolos, A., Emmanouil, C., Tsiridis, V., Tsiropoulos, N., 2009. Evaluation of toxic and interactive toxic effects of three agrochemicals and copper using a battery of microbiotests. Sci. Total. Environ. 407 (16), 4610–4615.

Larsson, S., Reimann, A., Nilvebrant, N.-O., Jönsson, L.J., 1999. Comparison of different methods for the detoxification of lignocellulose hydrolyzates of spruce. Appl. Biochem. Biotechnol. 77 (1), 91–103.

Lin, Y.H., Hwang, S.C.J., Gong, J.T., Wu, J.Y., Chen, K.C., 2005. Using redox potential to detect microbial activities during clavulanic acid biosynthesis in *streptomyces clavuligerus*. Biotechnol. Lett. 27 (22), 1791.

Liu, Y., Zhou, H., Wang, L., Wang, S., Fan, L., 2016. Improving *Saccharomyces cerevisiae* growth against lignocellulose-derived inhibitors as well as maximizing ethanol production by a combination proposal of γ-irradiation pretreatment with in situ detoxification. Chem. Eng. J. 287, 302–312.

Lopez-Hidalgo, A.M., Sánchez, A., De León-Rodríguez, A., 2017. Simultaneous production of bioethanol and biohydrogen by *Escherichia coli WDHL* using wheat straw hydrolysate as substrate. Fuel 188, 19–27.

Masand, V.H., El-Sayed, N.N.E., Mahajan, D.T., Mercader, A.G., Alafeefy, A.M., Shibi, I.G., 2017. QSAR modeling for anti-human African trypanosomiasis activity of substituted 2-phenylimidazopyridines. J. Mol. Struct. 1130, 711–718.

Meng-Lund, H., Kasten, G., Jensen, K.T., Poso, A., Pantsar, T., Rades, T., Rantanen, J., Grohganz, H., 2018. The use of molecular descriptors in the development of co-amorphous formulations. Eur. J. Pharm. Sci. 119, 31–38.

Mills, T.Y., Sandoval, N.R., Gill, R.T., 2009. Cellulosic hydrolysate toxicity and tolerance mechanisms in *Escherichia coli*. Biotechnol. Biofuels 2 (1) 26-26.

Nirmalakhandan, N., Xu, S., Trevizo, C., Brennan, R., Peace, J., 1997. Additivity in microbial toxicity of nonuniform mixtures of organic chemicals. Ecotoxicol. Environ. Saf. 37 (1), 97–102.

Palmqvist, E., Hahn-Hägerdal, B., 2000. Fermentation of lignocellulosic hydrolysates. II: inhibitors and mechanisms of inhibition. Bioresour. Technol. 74 (1), 25–33.

Roy, K., Das, R.N., 2013. QSTR with extended topochemical atom (ETA) indices. 16. Development of predictive classification and regression models for toxicity of ionic liquids towards *Daphnia magna*. J. Hazard. Mater. 254–255, 166–178.

Saha, K., Maharana, A., Sikder, J., Chakraborty, S., Curcio, S., Drioli, E., 2019. Continuous

production of bioethanol from sugarcane bagasse and downstream purification using membrane integrated bioreactor. Catal. Today 331, 68–77.
Saravanakumar, T., Park, H.-S., Mo, A.-Y., Choi, M.-S., Kim, D.-H., Park, S.-M., 2016. Detoxification of furanic and phenolic lignocellulose derived inhibitors of yeast using laccase immobilized on bacterial cellulosic nanofibers. J. Mol. Catal. B. Enzym. 134, 196–205.
Shen, G., Lu, Y., Hong, J., 2006. Combined effect of heavy metals and polycyclic aromatic hydrocarbons on urease activity in soil. Ecotoxicol. Environ. Saf. 63 (3), 474–480.
Shin, G.-J., Jeong, S.-Y., Lee, J.-W., 2017. Evaluation of antioxidant activity of the residues generated from ethanol concentration of lignocellulosic biomass using pervaporation. J. Ind. Eng. Chem. 52, 51–58.
Sizer, I.W., 1942. The activity of yeast invertase as a function of oxidation-reduction potential. J. Gen. Physiol. 25 (3), 399–409.
Stebbing, A.R.D., 2002. Tolerance and hormesis—increased resistance to copper in hydroids linked to hormesis. Mar. Environ. Res. 54 (3), 805–809.
Su, L., Xing, Y., MU, C., YAN, J., ZHAO, Y., 2008. Evaluation and QSAR study of joint toxicity of substituted phenols and cadmium to *Photobacterium phosphoreum*. Chem. Res. Chin. Univ. 24 (3), 281–284.
Su, L., Zhang, X., Yuan, X., Zhao, Y., Zhang, D., Qin, W., 2012. Evaluation of joint toxicity of nitroaromatic compounds and copper to *Photobacterium phosphoreum* and QSAR analysis. J. Hazard. Mater. 241–242, 450–455.
Su, L.M., Zhao, Y.H., Yuan, X., Mu, C.F., Wang, N., Yan, J.C., 2010. Evaluation of combined toxicity of phenols and lead to *Photobacterium phosphoreum* and quantitative structure-activity relationships. B. Environ. Contam. Tox. 84 (3), 311.
Szambelan, K., Nowak, J., Frankowski, J., Szwengiel, A., Jeleń, H., Burczyk, H., 2018. The comprehensive analysis of sorghum cultivated in Poland for energy purposes: separate hydrolysis and fermentation and simultaneous saccharification and fermentation methods and their impact on bioethanol effectiveness and volatile by-products from the grain and the energy potential of sorghum straw. Bioresour. Technol. 250, 750–757.
Tang, J., Wang, X.C., Hu, Y., Zhang, Y., Li, Y., 2017. Effect of pH on lactic acid production from acidogenic fermentation of food waste with different types of inocula. Bioresour. Technol. 224, 544–552.
Tugcu, G., Ertürk, M.D., Saçan, M.T., 2017. On the aquatic toxicity of substituted phenols to *Chlorella vulgaris*: QSTR with an extended novel data set and interspecies models. J. Hazard. Mater. 339, 122–130.
van Dijken, J.P., Scheffers, W.A., 1986. Redox balances in the metabolism of sugars by yeasts. Fems Microbiol. Lett. 32 (3), 199–224.
Wang, D., Wu, X., Lin, Z., Ding, Y., 2018. A comparative study on the binary and ternary mixture toxicity of antibiotics towards three bacteria based on QSAR investigation. Environ. Res. 162, 127–134.
Wang, X., Tsang, Y.F., Li, Y., Ma, X., Cui, S., Zhang, T.-A., Hu, J., Gao, M.-T., 2017. Inhibitory effects of phenolic compounds of rice straw formed by saccharification during ethanol fermentation by *Pichia stipitis*. Bioresour. Technol. 244, 1059–1067.
Wu, Y., Ma, H., Zheng, M., Wang, K., 2015. Lactic acid production from acidogenic fermentation of fruit and vegetable wastes. Bioresour. Technol. 191, 53–58.
Xu, S., Nirmalakhandan, N., 1998. Use of QSAR models in predicting joint effects in multicomponent mixtures of organic chemicals. Water. Res. 32 (8), 2391–2399.
Yong-Ling Wu, D.-L.W., Guo, En-Hui, Song, Shuang, Feng, Jun-Tao, Zhang, Xing, 2017. Synthesis and QSAR study of novel α-methylene-γ-butyrolactone derivatives as antifungal agents. Bioorg. Med. Chem. Lett. 27 (5), 1284–1290.
Zaldivar, J., Martinez, A., Ingram, L.O., 2000. Effect of alcohol compounds found in hemicellulose hydrolysate on the growth and fermentation of ethanologenic *Escherichia coli*. Biotechnol. Bioeng. 68 (5), 524–530.
Zhang, Q., Huang, H., Han, H., Qiu, Z., Achal, V., 2017. Stimulatory effect of in-situ detoxification on bioethanol production by rice straw. Energy 135, 32–39.
Zhao, X., Moates, G.K., Elliston, A., Wilson, D.R., Coleman, M.J., Waldron, K.W., 2015. Simultaneous saccharification and fermentation of steam exploded duckweed: improvement of the ethanol yield by increasing yeast titre. Bioresour. Technol. 194, 263–269.